Expression of 25 Human ABC Transporters in the Yeast *Pichia pastoris* and Characterization of the Purified ABCC3 ATPase Activity[†]

Maja Chloupková,[‡,§] Amanda Pickert,[‡] Jyh-Yeuan Lee,[‡] Shiloe Souza,[‡] Yenphuong T. Trinh,[‡] Sara M. Connelly,[||] Mark E. Dumont,[||] Michael Dean,[⊥] and Ina L. Urbatsch*[,‡]

Department of Cell Biology and Biochemistry, Texas Tech University Health Sciences Center, Lubbock, Texas 79430, Department of Biochemistry and Biophysics, University of Rochester Medical Center, Rochester, New York 14642, and Laboratory of Genomic Diversity, NCI Frederick, Frederick, Maryland 21702

Received January 4, 2007; Revised Manuscript Received May 12, 2007

ABSTRACT: Human ATP-binding cassette (ABC) transporters comprise a family of 48 membrane-spanning transport proteins, many of which are associated with genetic diseases or multidrug resistance of cancers. In this study, we present a comprehensive approach for the cloning, expression, and purification of human ABC transporters in the yeast *Pichia pastoris*. We analyzed the expression of 25 proteins and demonstrate that 11 transporters, including ABCC3, ABCB6, ABCD1, ABCG1, ABCG4, ABCG5, ABCG8, ABCE1, ABCF1, ABCF2, and ABCF3, were expressed at high levels comparable to that of ABCB1 (P-glycoprotein). As an example of the purification strategy via tandem affinity chromatography, we purified ABCC3 (MRP3) whose role in the transport of anticancer drugs, bile acids, and glucuronides has been controversial. The yield of ABCC3 was 3.5 mg/100 g of cells in six independent purifications. Purified ABCC3, activated with PC lipids, exhibited significant ATPase activity with a V_{max} of 82 ± 32 nmol min^{-1} mg^{-1}. The ATPase activity was stimulated by bile acids and glucuronide conjugates, reaching 170 ± 28 nmol min^{-1} mg^{-1}, but was not stimulated by a variety of anticancer drugs. The glucuronide conjugates ethinylestradiol-3-glucuronide and 17β-estradiol-17-glucuronide stimulated the ATPase with relatively high affinities (apparent K_m values of 2 and 3 μM, respectively) in contrast to bile acids (apparent K_m values of >130 μM), suggesting that glucuronides are the preferred substrates for this transporter. Overall, the availability of a purification system for the production of large quantities of active transporters presents a major step not only toward understanding the role of ABCC3 but also toward future structure−function analysis of other human ABC transporters.

ATP-binding cassette (ABC) transporters constitute the largest family of membrane transport proteins and are ubiquitous in all kingdoms of life. In humans, 48 members of this family have been identified to date (*1*). On the basis of sequence similarities, domain organization, and phylogenetic analysis, the ABC transporters have been assigned to several subgroups, A−G. In general, a functional transporter consists of two soluble nucleotide-binding domains (NBDs) that power the transport reaction by hydrolyzing ATP and two transmembrane domains (TMDs) that harbor a translocation pathway for a particular substrate (*2*). Human ABCs are either full-size transporters with all four domains encoded by the same gene (TMD−NBD−TMD−NBD) or half-size transporters with one NBD and one TMD (NBD−TMD or TMD−NBD) expressed from the same gene; half-size transporters homo- or heterodimerize to form a functional unit. The exceptions from this domain organization are members of the subfamilies E and F, which consist of two fused NBDs and lack the TMDs. The NBDs are highly conserved among all ABC transporters. They contain the classic Walker A and B motifs that are characteristic of ATP-hydrolyzing enzymes, a short "ABC signature" sequence, LSGGQ, specific to ABC proteins, and several conserved structural loops termed D, H, and Q loops (*3*). In contrast, the TMDs of ABC transporters exhibit only weak sequence similarity. Presumably as a result of this diversity, the nature of transport substrates ranges from chloride (ABCC7 or CFTR) or metal (ABCB7) ions and antigenic peptides (ABCB2/B3 or TAP1/TAP2) to large hydrophobic compounds (ABCB1 and ABCC1), lipids (ABCB4 and ABCC2), and cholesterol (ABCA1 and ABCG5/G8) (*1*).

Consistent with the wide spectrum of substrate molecules and their variable biological functions, the phenotypes associated with human ABC transporters are extremely diverse. Eighteen ABC transporters have been associated with human disorders so far (*1*), including cystic fibrosis

[†] This work was supported mainly by Start-up funds from the Texas Tech University Health Sciences Center as well as by the American Heart Association, Texas, the South Plains Foundation (Lubbock, TX), the Helen Jones Foundation (Lubbock, TX), and the Wilson Foundation (Dallas, TX) (to I.L.U.) and was supported in part by the Intramural Research Program of the NIH, National Cancer Institute, Center for Cancer Research (to M.D.) and National Institutes of Health Grant P50 GM64655 (Wim Hol, principal investigator; subcontract to M.E.D.).

* To whom correspondence should be addressed: Department of Cell Biology and Biochemistry, Texas Tech University Health Sciences Center, Lubbock, TX 79430-6540. Phone: (806) 743-1192. Fax: (806) 743-2990. E-mail: ina.urbatsch@ttuhsc.edu.

[‡] Texas Tech University Health Sciences Center.

[§] Current address: Department of Cell and Developmental Biology, Oregon Health and Science University, Portland, OR 97239.

[||] University of Rochester Medical Center.

[⊥] NCI Frederick.

10.1021/bi700020m CCC: $37.00
Published on Web 06/15/2007

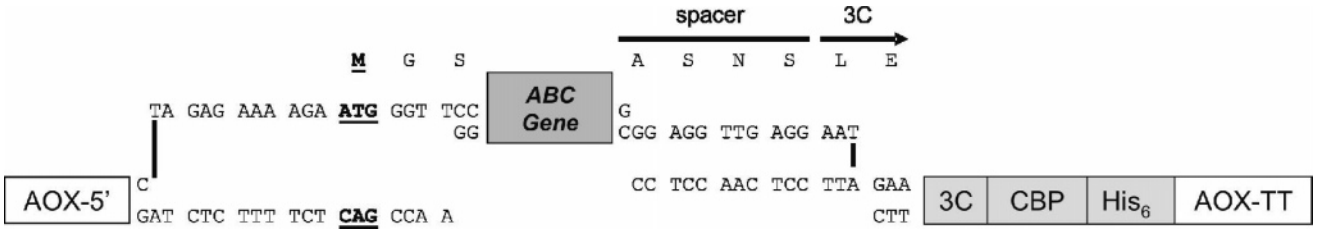

FIGURE 1: High-throughput cloning strategy of human ABC transporters for expression in *P. pastoris*. Schematic representation of the expression construct for ligation-independent cloning (LIC). Single-stranded overhangs, produced by the 3′ to 5′ exonuclease reactivity of T4 DNA polymerase in the presence of dGTP and dCTP, respectively, are shown for the PCR-amplified gene (top) and the corresponding counterparts in the vector (bottom). After cloning, the pSGP18 plasmid encodes a protein bearing a C-terminal 3C-protease cleavage site (3C), a calmodulin binding peptide (CBP), and an RGS-His_6 tag. In addition, the vector contains Kozak-like bases in the region around the ATG start codon (positions −3 and +1) important for high-level expression in *P. pastoris* (*29*).

(*4*), immunodeficiency (*5*), blindness (*6*), neurodegeneration (*7*), pulmonary defects (*8*), and defects in lipid and cholesterol metabolic pathways (*8*, *9*). In addition, several transporters account for multidrug resistance of tumor cells that complicates treatments of patients with various types of cancers (*10*, *11*). However, the precise biological roles of many ABC transporters remain unknown, even in cases where mutations in the transporter are associated with a human phenotype(s).

In recent years, substantial efforts to understand the structure−function relationships of this family of transporters have been made. X-ray structures of the isolated soluble NBDs have been determined at high resolution for many ABC transporters, including one of the NBDs of human ABCC7 (CFTR) and ABCB2 (TAP1) (reviewed in ref *12*). However, despite this effort, X-ray structures that include the TMDs are available so far for only four half-size transporters from bacteria (*13*−*16*), and only low-resolution, electron microscopy structures have been obtained for human full-size transporters (*17*−*21*). Moreover, only a few human ABC transporter have been extensively characterized in terms of ATPase activity and transport specificity (*4*, *5*, *22*, *23*). The main reason for a relatively slow progress in the field of human ABC transporters is the difficulty in expressing significant quantities of active forms of these hydrophobic proteins. An excellent example is ABCB1 [P-glycoprotein (Pgp)] which has been expressed in various organisms (*24*−*27*). However, the most economical system for producing sufficient quantities of the active wild-type transporter and its mutant variants for further biochemical and biophysical analyses has proven to be the yeast *Pichia pastoris* (*28*−*30*).

Previous studies of expression and purification of human ABC transporters have consisted of one-at-a-time efforts to investigate particular proteins. The first goal of this study was to capitalize on experience gained through studies of ABCB1 (Pgp) in *P. pastoris* and develop a high-throughput system to allow efficient cloning, expression, and purification of the human ABC transporter. Thus, we present the expression profile for 25 human ABC transporters in *P. pastoris*. As an example of the usefulness of this approach for purification and further biochemical characterization of transporters, we have focused on the ABCC3 (MRP3) protein. ABCC3 was originally expected to transport a broad spectrum of anticancer drugs and to contribute to the multidrug resistance of human cancers, based on the fact that it is a member of the family of multidrug resistance (MDR) ABC transporters. The protein is overexpressed in patients with cholestasis and has therefore been suggested to function as an escape route for bile acids under conditions of impaired bile flow (*31*). However, its normal biological role in the transport of bile acids and perhaps glucuronide conjugates is still under active investigation (*32*). Thus, the second goal of this study was to address the substrate specificity of purified ABCC3.

MATERIALS AND METHODS

Materials. PfuUltra was from Stratagene, and T4 DNA polymerase was from Novagen. *n*-Dodecyl β-D-maltopyranoside (DDM)[1] and other detergents were obtained from Anatrace. Ni^{2+}-NTA agarose resin was from Qiagen (Valencia, CA), and calmodulin affinity resin was from Stratagene (La Jolla, CA). Asolectin (crude soybean phospholipids) was from Sigma (St. Louis, MO), and all other lipids (acetone/ether-precipitated preparations) were from Avanti Polar Lipids (Alabaster, AL). Bile acids, $E_2$17βG, and morphine glucuronide were from Sigma, and acetaminophen-G, ethinylestradiol-G, and ethinylestradiol-S were from Steraloids (Newport, RI).

Cloning and Expression of Human ABC Transporters. The *P. pastoris* expression vectors pSGP17 and pSGP18 were derived from pPICZαB (Invitrogen) by insertion of a new translational start site, the sequences allowing rapid insertion of reading frames via ligation-independent cloning (*33*), and a C-terminal tag consisting of a cleavage site for rhinovirus 3C protease followed by calmodulin binding peptide and a six-His sequence (S. M. Connelly, N. Fedoriw, K. M. Clark, K. Robinson, E. Walker, I. Urbatsch, and M. Dumont, manuscript in preparation). Vector pSGP17 contained the pre-pro-α-factor leader sequence from pPICZαB in addition to cloning and tag sequences identical to those of pSGP18. The inserted sequences were assembled using overlapping synthetic oligonucleotides and inserted between either *Bst*BI and *Sal*I sites or *Bsr*DI and *Sal*I sites in pPICZαB. Insertion of reading frames into these vectors for expression is accomplished by cleavage of pSGP18 (Figure 1) with *Bsm*BI, an enzyme that cleaves outside of its recognition sequence, followed by treatment of the cut vector with T4 DNA polymerase in the presence of dCTP. In the case of

[1] Abbreviations: DDM, *n*-dodecyl β-D-maltopyranoside; DTT, dithiothreonine; PMSF, phenylmethanesulfonyl fluoride; GSH, glutathione; AG, acetaminophen-G; MG, morphine-G; E217βG, 17β-estradiol-17β-D-G; EEG, ethinylestradiol-3G; EE-S, ethinylestradiol-3-sulfate; PC lipids, L-α-phosphatidylcholine; DOPC, 1,2-dioleoyl-*sn*-glycero-3-phosphocholine.

pSGP18, this procedure leads to insertion of the sequence Met-Gly-Ser prior to the second amino acid of each reading frame (Figure 1). In the case of pSGP17, each reading frame contains the pre-pro-α-factor sequence followed by Met-Gly-Ser prior to the second amino acid.

cDNAs encoding the full-length human ABC transporter genes were kindly provided by P. Borst (ABCC2 and ABCC3), G. Kruh (ABCC5 and ABCC6), and I. Pastan (ABCC12). The remaining cDNAs were obtained from the National Institutes of Health collection (M. Dean). Individual ORFs were amplified by PCR using PfuUltra polymerase and oligonucleotide primers providing 5′ sequences (AGAGAAAAGAATGGGTTCC) and 3′ sequences (TAAGGAGTTGGAGGC) for ligation-independent cloning (Figure 1). PCR products were treated with T4 DNA polymerase in the presence of dGTP, incubated with cut and T4-treated vector as described previously (*33*−*35*), and then transformed into XLI-blue cells (Novagen). The integrity of the individual ORFs in the expression plasmids was confirmed by DNA sequencing.

Individual plasmids were transformed into *P. pastoris* strain KM71 by electroporation following standard procedures (http://www.invitrogen.com/content/sfs/manuals/easyselect_man.pdf). Transformants were plated on YPDS containing 100, 500, or 1000 μg/mL zeocin to select for single-copy and multicopy integrations. For protein expression analysis, several transformants from each plate were grown and induced with methanol in 10 mL cultures as previously described (*28*, *36*) with inclusion of 0.004% histidine in the medium. "Rapid Membranes" were prepared (*28*), and 15 μg of microsomal membranes was resolved by SDS−PAGE followed by Western blot analysis. For immunodetection, monoclonal anti-RGS-His_4 antibody (Qiagen) was used with the TMB substrate system (Kirkegaard & Perry). The TMB substrate is less sensitive than ECL but gives more consistent staining intensities for easy comparison between blots.

Growth of Fermentor Cultures and Preparation of Microsomes. The fermentation of *P. pastoris* cultures was conducted as described previously (*28*). From a 5 L fermentor culture, 1.3−1.5 kg of cells was harvested, and they were frozen at −80 °C in 100 g batches as described previously (*37*). Cells were disrupted in a Bead Beater, and microsomal membranes were prepared (*37*). The yield of microsomes was ∼400 mg per 100 g of wet weight cells.

Solubilization Trials. For small-scale solubilization trials, microsomal membranes were diluted to 4 mg/mL in buffer A [50 mM Tris-HCl (pH 7.4), 50 mM NaCl, and 30% glycerol] supplemented with protease inhibitors (10 μg/mL leupeptin, 10 μg/mL pepstatin A, 2.5 μg/mL chymostatin, and 1 mM PMSF). Aliquots of 30 μg (7.5 μL) were mixed with an equal volume of detergent solution in buffer A to give a final detergent concentration of 1% (w/v). Protein/detergent mixtures were incubated for 10 min at room temperature, and insoluble material was removed by centrifugation at 64000*g* for 30 min at 4 °C. The soluble supernatants were resolved by SDS−PAGE, and the relative staining intensities were determined by Western blot analysis.

Purification of ABCC3. Purification of ABCC3 followed the same procedure that is described in ref *37* except that the microsomes were solubilized in 0.6% DDM and the detergent concentration was reduced to 0.1% DDM during chromatography on Ni-NTA and calmodulin resins. Purified ABCC3 was concentrated by ultrafiltration under N_2 using an Amicon stirred cell with an XM-50 membrane (Millipore) to 1−2 mL, and the protein concentration was determined by UV spectroscopy using a calculated A_{280}(1 mg/mL) of 1.31 for ABCC3. The concentrated material was aliquoted and stored at −80 °C.

Activation of Purified ABCC3 by Lipids. Lipid stocks were made from *Escherichia coli* lipids, liver lipids, egg PC lipids, or asolectin at a final concentration of 20 mg of lipid/mL as described previously (*28*) and stored under N_2. For activation experiments, detergent-soluble protein was mixed with an equal volume of lipids and incubated at room temperature for 20 min and then sonicated in a bath sonicator at room temperature for 30 s. The protein was stored on ice for a minimum period of time until the assay.

ATPase Assays. ATPase assays and assessment of the release of inorganic phosphate were performed as described previously (*37*). For determination of kinetic parameters, MgATP concentrations were varied with an excess of 2 mM Mg^{2+} over ATP in each tube. Tested substrates were added from stocks in dimethyl sulfoxide with the final concentration of the solvent being ≤2% (v/v) in the assays. Stimulation of ATPase activity was conducted as indicated in the figure legends for individual experiments. The data in Figures 5B and 6B were fitted to the Hill equation, $f = a + (bx^c)/(d^c x^c)$, using SigmaPlot 8.0, where a is the basal activity, b is the maximum activity, x is the substrate concentration, c is the Hill coefficient, and d is the apparent K_m. Inhibition by phosphate analogues was assayed in cocktails containing 10 mM MgATP supplemented with 1 or 3 mM orthovanadate and $BeSO_4$ with 5 mM NaF (BeFx) or $AlCl_3$ with 5 mM NaF (AlFx). Orthovanadate solutions (100 mM) were prepared from Na_3VO_4 (Fisher Scientific) at pH 10 and boiled for 2 min before each use to break down polymeric species (*37*).

Routine Procedures. Protein concentrations of microsomal membranes were determined via a Bradford assay (Bio-Rad). SDS−PAGE was performed using a Mini-PROTEAN-3 gel and Electrotransfer system (Bio-Rad). Samples were dissolved in 0.5 volume of sample buffer [125 mM Tris-HCl (pH 6.8), 5% (w/v) SDS, 25% (v/v) glycerol, 0.01% pyronin Y, and 160 mM DTT] for 20 min at 37 °C and then resolved on 10% polyacrylamide gels.

RESULTS

Cloning and Expression of Human ABC Transporters. We have examined expression of ABC transporters using a new vector, pSGP18, designed for the expression of membrane proteins in the yeast *P. pastoris* for structural genomic applications. This vector allows insertion of target open reading frames via ligation-independent cloning (LIC), a procedure that permits directional cloning of PCR products without the need for restriction enzyme digestion or ligation reactions (*33*). In this approach, vectors and PCR-amplified ORFs are treated with T4 DNA polymerase in the presence of only one dNTP to produce specific 14−18-base single-stranded overhangs via its 3′ to 5′ exonuclease reactivity. The LIC vector and insert are then annealed and introduced into competent *E. coli* cells to yield a circular plasmid. Proteins cloned into pSGP18 are expressed under the control of the strong, inducible *AOX1* promoter and are fused to in-

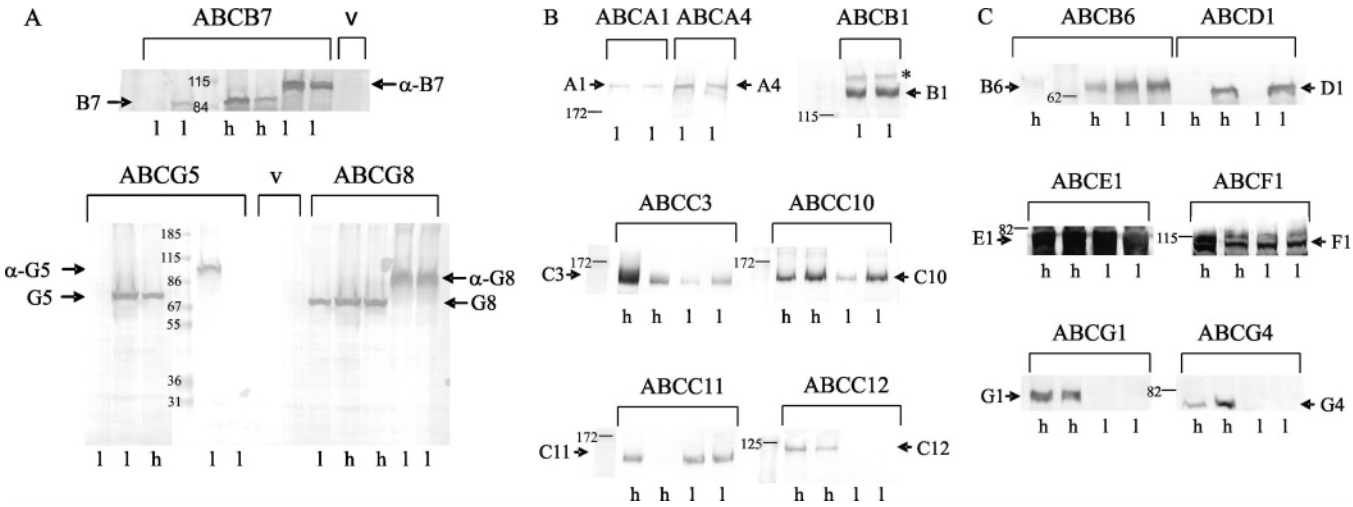

FIGURE 2: Expression analysis of ABC transporters. Membrane preparations of *P. pastoris* transformants (see Materials and Methods) were resolved via SDS−PAGE and analyzed on Western blots using a monoclonal antibody against the C-terminal RGS-His_4 epitope. The names of the respective gene products are given at the top of the blots. Vector lanes (v) are from control cells transformed with the "empty" vector and are not expected to cross-react with the antibody. Transformants marked "l" and "h" were selected on low (100 μg/mL) and high (1000 μg/mL) concentrations of zeocin, respectively. For the sake of simplicity, a representative blot, which includes the entire panel of molecular mass (MW) protein markers, is shown only for the ABCG5 and ABCG8 transporters (panel A). The same MW protein markers were used on all blots and are indicated in kilodaltons. For direct comparison of the levels of individual transporters, equal amounts of protein (15 μg) were loaded in each lane. In the case of very strong expression (ABCE1 or ABCF subfamily), the signal appeared as "overloading", while in the case of very weak expression (ABCA1), the immunological signal was barely visible. (A) Half-size transporters expressed from both pSGP18 and pSGP17 vectors. Calculated molecular masses of the recombinant ABCB7, ABCG5, and ABCG8, including the C-terminal affinity tags, are 89, 82, and 79 kDa, respectively. The presence of the pre-pro-α-factor leader sequence adds 8.9 kDa to each protein. Protein bands on Western blots corresponding to the protein containing the pre-pro-α-factor leader sequence (unprocessed) showed slower mobility (two rightmost lanes of each transporter) and are designated with the prefix "α". Similar mobility shifts were seen for ABCF2 and ABCF3 (not shown). (B) Full-length transporters expressed from pSGP18. Calculated molecular masses of the recombinant ABCA1, ABCA4, ABCB1, ABCC3, ABCC10, ABCC11, and ABCC12 proteins are 253, 262, 147, 176, 165, 161, and 120 kDa, respectively. The asterisk denotes that ABCB1 forms inter- and intramolecular disulfides explaining the occurrence of several bands seen on the blot (*29*). (C) Half-size transporters expressed from pSGP18. Calculated molecular masses of ABCB6, ABCD1, ABCE1, ABCF1, ABCG1, and ABCG4 are 100, 89, 74, 102, 80, and 78 kDa, respectively. The expression of ABCC1 in *P. pastoris* had already been reported (*62*), and thus, its expression was excluded from this study.

frame C-terminal sequences encoding a four-amino acid spacer, a recognition sequence for rhinovirus 3C protease, and a tandem affinity purification tag composed of a calmodulin binding peptide and an RGS-His_6 epitope that is recognized by a monoclonal anti-RGS-His_4 antibody, allowing for immunologic detection of the expressed proteins (Figure 1). In addition, we generated a derivative of this vector, pSGP17, that contains an additional N-terminal signal sequence derived from *Saccharomyces cerevisiae* pre-pro-α-factor (see Materials and Methods) to determine whether the presence of such a signal might promote targeting of the proteins to the plasma membrane and enhance levels of expression of the active protein.

We first cloned P-glycoprotein (Pgp, ABCB1) into both pSGP17 and pSGP18 to compare expression levels in these new vectors with the expression level in the previously tested pHIL-D2 vector (*29*). Individual expression plasmids were transformed into *P. pastoris* cells and transformants selected on plates containing increasing concentrations of zeocin (see Materials and Methods). Eight transformants of each gene were analyzed for protein expression on Western blots (Figure S1 of the Supporting Information). Of these, six (pSGP18) and seven (pSGP17) transformants revealed a protein band of the expected size that cross-reacted with a Pgp-specific antibody. The expression levels, as reflected by the staining intensities of the Pgp bands, were very similar among transformants produced in pSGP18 (lanes 1−4), pSGP17 (lanes 5−8), and pHIL-D2 (lanes 10 and 11) vectors. This indicates that the longer C-terminal tag in pSGP17 and pSGP18 than in pHIL-D2 did not compromise protein production in *P. pastoris*. Pgp protein expressed in the pSGP17 vector, however, migrated slower than its pSGP18 counterpart (Figure S1, lanes 5−8 vs lanes 1−4) as might be expected if the leader sequence was not effectively cleaved by the endogenous signal peptidase. Similar differences in size between pSGP17 and pSGP18 counterparts were observed for five other gene products (see below, Figure 2A). The use of the pSGP17 vector was thus not pursued further.

In addition to ABCB1 (Pgp), we cloned 25 of the 48 human ABC transporters into pSGP18 and analyzed their expression in *P. pastoris*. All full-size ABC transporters that were detected on Western blots using the anti-RGS-His_4 antibody are shown in Figure 2B; half-size transporters are shown in panels A and C of Figure 2. To compare the relative expression levels of various transporters, Pgp (ABCB1) was used as an internal reference (Figure 2B, top right panel). The results of the Western blot analysis, which are summarized in Table S1, revealed the following. (i) More than 50% of the tested proteins were expressed at detectable levels in *P. pastoris*. (ii) Shorter gene products were more readily expressed than longer ones. For example, only two of the five large gene products analyzed in the A subfamily could be detected on Western blots (Figure 2B, top left), while four of the five half-size transporters in the G subfamily were expressed at levels comparable to that of ABCB1 (Figure 2A,C, bottom panels). (iii) Expression levels varied between transformants of the same gene and did not always correlate with their resistance to zeocin, which was used to select for

multicopy integrations of the recombinant genes into the *P. pastoris* chromosome. Interestingly, ABCC12, ABCG1, and ABCG4 proteins were detected only in transformants selected with high concentrations of zeocin, while the expression level of ABCB6 (Figure 2C) was somewhat higher in transformants selected with a low zeocin concentration; the expression levels of ABCC10, ABCC11, and ABCD1 were independent of the zeocin concentration. Yeast transformants of plasmids expressing ABCA1, ABCA4, and ABCB1 were obtained with only low concentrations of zeocin in repeated experiments. The reason for this behavior is not clear but may reflect toxic effects of expression of larger gene products from multicopy integration events, since we obtained highly zeocin-resistant transformants for all of the half-size transporters. (iv) When a particular expressed protein was detected at all by immunoblotting, expression was detected in two or three of four independent transformants. However, we did not detect any signal for ABCC2 on Western blots among the 12 transformants that were screened. In the case of ABCC6, we did not detect any full-length protein in 14 transformants that were analyzed, although smaller products were visible in some of them (data not shown), indicating that proteolytic degradation during cell growth and subsequent manipulations might be one of the factors limiting the expression of a particular transporter.

In summary, the full-size transporter that exhibited the best expression was ABCC3. Among the half-size transporters, several proteins were expressed at levels similar to or higher than that of Pgp, including ABCB6, ABCD1, ABCG1, ABCG4, ABCG5, and ABCG8. Interestingly, members of the E and F subfamilies, which are predicted to consist of two fused soluble NBDs, gave very strong signals on Western blots. Their high expression levels might reflect their hydrophilic nature since they lack the typical transmembrane domains normally present in the human ABC transporters (*1*).

Solubilization and Purification of ABCC3. Because of our interest in transporters of the liver and gut, and because of its high level of expression, we chose the full-size transporter ABCC3 for further studies, including solubilization, purification, and functional analyses in our system. A microsomal membrane fraction was isolated from fermentor cultures of the best-expressing clone of ABCC3 (Figure 2B) to collect proteins present in plasma membranes and in intracellular membranes (*28*). The solubility of ABCC3 was tested in a variety of detergents that were selected on the basis of their previous use for the purification of highly active P-glycoprotein (MDR1, ABCB1) (*29*) and for the purification of other membrane proteins (http://blanco.biomol.uci.edu/membrane_proteins_xtal.html). Although many detergents were efficient in the extraction of ABCC3 from the membranes (Figure 3A), the most efficient and reproducible extraction of ABCC3 was obtained with *n*-dodecyl β-D-maltopyranoside (DDM), which was then selected for large-scale purifications.

Following a purification procedure based on methods successfully applied to the purification of Pgp from *P. pastoris* membranes (*29*), ABCC3 was solubilized in DDM and purified by tandem affinity chromatography on Ni-NTA and calmodulin affinity resin (see Materials and Methods). An SDS gel following the progress of the purification is shown in Figure 3B. Approximately ~3.5 mg of highly purified (>90%) protein was obtained from 100 g of yeast cells in six independent purifications (Table 1). The purified material remained stably soluble in buffers with low concentrations (0.1%, w/v) of DDM.

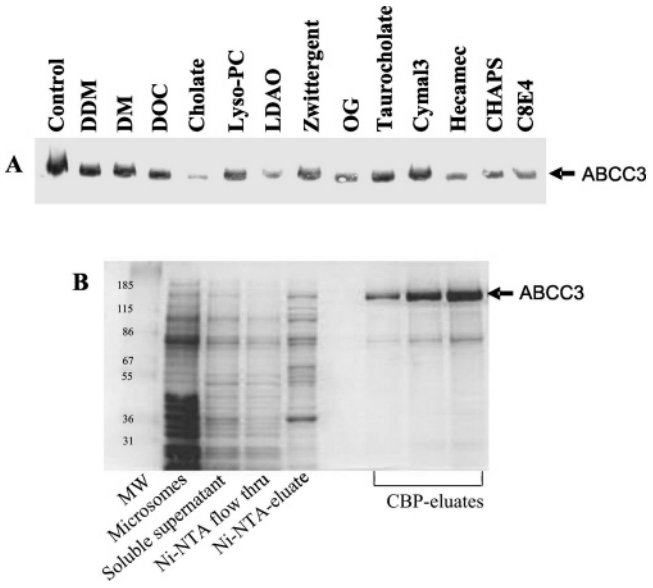

FIGURE 3: Extraction and purification of ABCC3 from microsomal membranes. (A) Solubility in various detergents. Thirty micrograms of microsomal membranes (2 mg/mL) was incubated with the detergents at a final concentration of 1% as indicated above the Western blot for 10 min at room temperature. The insoluble material was then removed by centrifugation at 63000*g* for 30 min at 4 °C, and the detergent extracts were resolved on SDS gels followed by Western blotting. (B) Progress of the purification in DDM after consecutive chromatography on Ni-NTA and calmodulin (CBP) resins. Protein samples were resolved on a SDS−PAGE gel followed by Coomassie Blue staining. Increasing amounts (3, 6, and 9 μg) of the final purified and concentrated ABCC3 that eluted from the calmodulin resin (CBP eluates) are shown. Positions of the MW protein markers are indicated in kilodaltons. The slight impurity around 80 kDa did not cross-react with the RGS-His antibody or an ABCC3-specific N-terminal antibody (Santa Cruz Biotechnology, Inc.).

Table 1: Purification and ATPase Activity of ABCC3

	yield (mg of protein/ 100 g of cells)	no. of purifications	ATPase activity (nmol min^{-1} mg^{-1})	K_m(MgATP) (mM)	K_{cat}/K_m (M^{-1} s^{-1})
ABCC3	3.5	6	82 ± 32^a	2.1	115
			$170 \pm 28^{a,b}$	2.0	249
			175 ± 20^c	1.9	270

[a] ATPase activity was determined at 20 mM MgATP. The mean and standard deviation of at least 45 independent assays, including all six purified ABCC3 preparations, are given. [b] ATPase activity was determined in the presence of 1 mM taurocholate. [c] ATPase activity was determined in the presence of 10 μM ethinylestradiol-G.

ATP Hydrolysis of Purified ABCC3. ABC transporters are ATP-dependent membrane pumps. We therefore examined whether purified ABCC3 exhibits ATPase activity in the presence and absence of lipids (Figure 4). For this purpose, purified ABCC3 in detergent solution was activated with lipids from various sources and the ATPase activity assayed after dilution into cocktails containing 10 mM MgATP (see Materials and Methods). ATP hydrolysis was readily detected, and the amount of inorganic phosphate product was found to increase over time. In the absence of lipids, the ATP hydrolysis apparently slowed after ~10 min at 37 °C, indicating that the protein in detergent soluble form was

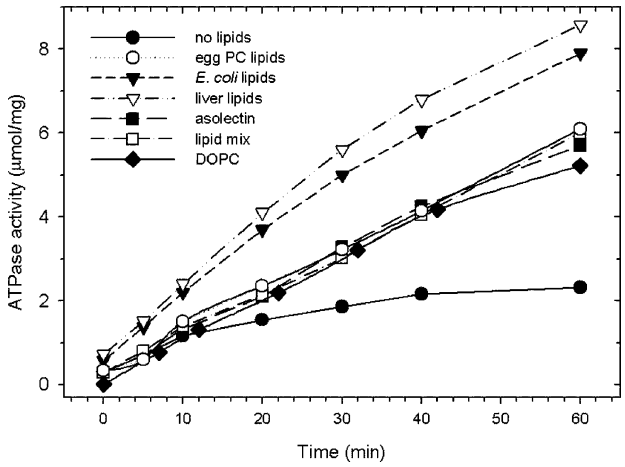

FIGURE 4: ATPase activity of ABCC3. Purified, detergent-soluble ABCC3 was either directly diluted into 10 mM MgATP cocktail or activated with 1% lipids for 20 min at room temperature followed by a 30 s sonication prior to dilution into an ATP cocktail. ATP hydrolysis was assayed for the indicated times at 37 °C and the amount of inorganic phosphate determined as described in Materials and Methods. Average values from four independent experiments are shown; standard deviations were small (<0.5 μmol/mg) and were omitted for the sake of clarity. "Lipid mix" is a mixture of phospholipids that resembles the plasma membrane composition more closely (*24*); DOPC is synthetic 1,2-dioleoyl-*sn*-glycero-3-phosphocholine.

somewhat unstable. The presence of any of the tested lipids led to a striking enhancement of enzyme activity, allowing rates of ATP hydrolysis to remain almost linear for up to 60 min. The highest specific ATPase activities were observed in the presence of liver and *E. coli* lipid. Slightly lower activities were detected in the presence of egg phosphatidylcholine (PC) lipids, asolectin, synthetic DOPC lipids, and a lipid mixture. Thus, we conclude that lipids in general have a stabilizing effect on ABCC3 consistent with the membrane location of the protein in vivo. Because of their defined composition and availability, we selected egg PC lipids (99% pure PC lipids) for further studies. The mean specific ATPase activity of ABCC3 derived from six independent purifications (>70 experiments), after activation with egg PC lipids, was 82 ± 32 nmol min^{-1} mg^{-1}. This is similar to the range of activities reported for other members of the ABCC subfamily, including the multidrug resistance-associated proteins ABCC1 [5−10 nmol min^{-1} mg^{-1} (*38*)] and ABCC2 [25 nmol min^{-1} mg^{-1} (*39*)], which are close relatives of ABCC3. A comparable activity has also been reported for another member of the C subfamily, the cystic fibrosis conductance regulator ABCC7 [CFTR, 60 nmol min^{-1} mg^{-1} (*19*, *40*)].

Effect of Various Potential Substrates on the ABCC3 ATPase Activity. Although the normal physiological transport substrates of ABCC3 remain to be determined, it has been demonstrated that ABCC3 in membrane vesicle systems can transport a variety of compounds such as bile salts and glucuronide conjugates (*32*) normally present in hepatocytes, as well as various anticancer drugs. Transport of these substrates by ABCC3 has been established to be strictly ATP dependent (reviewed in ref *32*), but rates of ATP hydrolysis have not yet been determined. Therefore, we determined whether the presence of these compounds leads to stimulation of the ATPase of ABCC3. To establish conditions for these assays, we first examined the effects of several bile acids on the ATPase activity of purified ABCC3 activated with

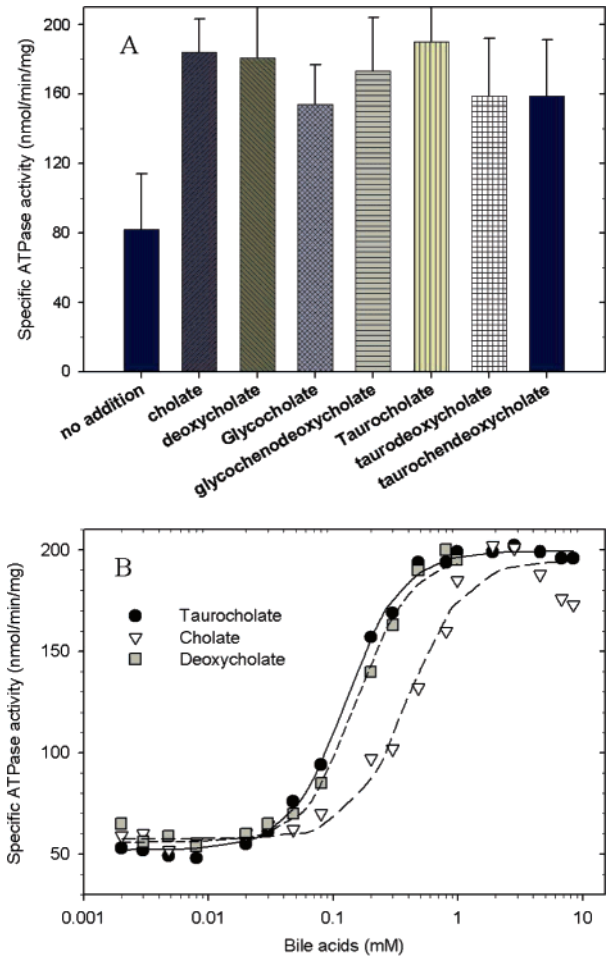

FIGURE 5: Stimulation and concentration dependence of the ABCC3 ATPase in the presence of bile acids. (A) Stimulation. ABCC3 was activated with egg PC lipids and ATPase activity assayed for 15 min at 37 °C in cocktails containing various bile acids. Bile salts were added from stocks in water (pH 7.4) to a final concentration of 1 mM. The bar graphs are the mean values obtained from at least three independent experiments ± standard deviations. (B) Concentration dependence. ATP hydrolysis was assayed as for panel A with increasing concentrations of bile salts. The solid and dashed lines in each case are fits to the Hill equation. The data are the averages of at least two independent experiments; standard deviations were small and were omitted for the sake of clarity.

different lipids. Maximal ATPase activity was similar in all bile acid−lipid combinations (~150−200 nmol min^{-1} mg^{-1}). However, the highest degree of stimulation was observed with egg PC lipids, since the basal activity (in the absence of added substrates) was lower with these lipids than with liver and *E. coli* lipids (data not shown). The latter two lipids are derived from tissue extracts and thus may contain variable amounts of endogenous ABCC3 substrates, accounting for the observed higher basal activity. Therefore, we selected egg PC lipids (>99% pure PC lipids) for further studies.

All bile acids that were tested significantly stimulated the ATPase activity of ABCC3 (Figure 5A). The highest ATPase activities of six different protein preparations were observed in the presence of taurocholate [170 ± 28 nmol min^{-1} mg^{-1}; n > 45 experiments (Table 1)]. Maximal activity was observed at concentrations of taurocholate greater than 1 mM (Figure 5B), and the concentration required for half-maximum stimulation (apparent K_m) was relatively high (~130 μM). Similar results were found for cholate and deoxycholate with apparent K_m values of 430 and 169 μM,

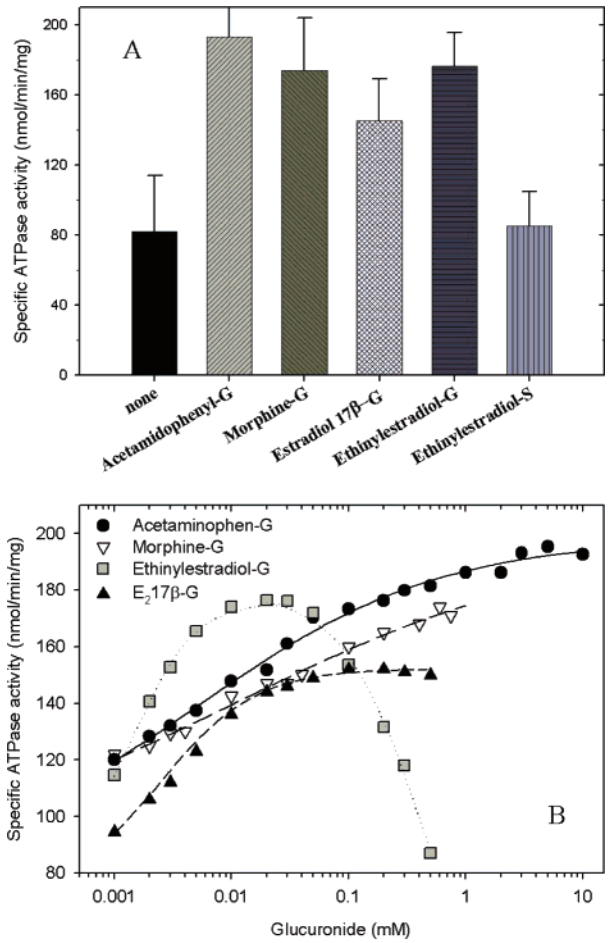

FIGURE 6: Stimulation and concentration dependence of the ABCC3 ATPase in the presence of glucuronides. (A) Stimulation. ATP hydrolysis was assayed as described in the legend of Figure 5. Glucuronides were added from stocks in DMSO to a final concentration of 100 μM ($E_2$17β-G), 5000 μM (acetamidophenyl-G), 800 μM (morphine-G), 10 μM (ethinylestradiol-G), and 20 μM (ethinylestradiol-S). GSH and DTT were added from stocks in water (pH 7.4) to a final concentration of 1 mM. The bar graphs are the mean values obtained from at least three independent experiments $\pm$ standard deviations. (B) Concentration dependence. ATP hydrolysis was assayed with increasing concentrations of glucuronides. The solid, dashed, and dotted lines in each case are fits to the Hill equation. Because of the shallow slope of the stimulation profile of acetaminophen-G (AG) and morphine-G (MG), the K_m could not be accurately determined. A direct fit to the Hill equation gave K_m values of 6 and 11 μM with Hill coefficients of 0.5 and 0.6 for AG and MG, respectively. A fit assuming two binding sites gave K_m(1) values of 1 and 3 μM and K_m(2) values of $>$50 and $>$100 μM for AG and MG, respectively. MG was not soluble at concentrations of $\geq$1 mM. The data are the averages of at least two independent experiments; standard deviations were small and were omitted for the sake of clarity.

respectively (Figure 5B). It is noteworthy that the slopes of all three activation curves in Figure 5B were steep; no stimulation of the ATPase was observed at bile salt concentrations of $\leq$50 μM. The best fit was obtained using the Hill equation (solid and dashed lines) with Hill coefficients of 1.9, 1.7, and 2.0 for taurocholate, cholate, and deoxycholate, respectively, suggesting that two binding sites are involved in the catalysis.

The glucuronide conjugates acetaminophen-G (AG), morphine-G (MG), 17β-estradiol-17β-D-G ($E_2$17βG), and ethinylestradiol-3G (EE-G) all stimulated ATPase activity (Figure 6A) with maximum specific activities similar to those observed in the presence of bile acids (Figure 5A). In contrast, the sulfate conjugate, ethinylestradiol-3S, had no effects on the ATPase. Interestingly, the stimulation profiles for AG and MG exhibited rather shallow slopes (Figure 6B), and the best fit to the data was obtained using the Hill equation (solid and dashed lines) with Hill coefficients of 0.52 and 0.45, respectively, suggestive of the existence of two binding sites for these compounds with negative cooperativity. An equally good fit was also obtained assuming two independent binding sites with significantly different affinities (see the figure legend). In the case of $E_2$17βG, no cooperativity was apparent, and a best fit was obtained with a Hill coefficient of $\sim$1 (short dashed line). For EE-G, the best fit was obtained using the Hill equation with a Hill coefficient of 1.7 (dotted line) which implies that two sites positively cooperate in binding of EE-G. The highest apparent affinities were found for $E_2$17βG and EE-G with apparent K_m values of 3 and 2 μM, respectively. Inhibition of ATPase activity of ABCC3 was observed at high concentrations of EE-G with an apparent K_i of 430 μM.

Because ABCC3, like other members of the ABCC subfamily, has been implicated in anticancer drug resistance (*41*), we analyzed the effects of a variety of known substrates of the multidrug resistance pumps ABCC1 (MRP1) and ABCB1 (Pgp) on the ATPase activity of ABCC3 (Figure 7). None of these compounds had a significant effect on ATP hydrolysis, indicating that they are poor substrates for ABCC3. In particular, it is remarkable that GSH had little effects on the ABCC3 activity, either alone or in combination with $E_2$17βG, etoposide, taurocholate, or glycocholate, since GSH significantly stimulate transport of other compounds by ABCC1 and is cotransported with these compounds (*23*, *42*). Thus, the substrate specificity of ABCC3 appears to be significantly different from that of its closest relative, the multidrug resistance-associated protein ABCC1 (MRP1), with whom it shares the highest degree of amino acid homology (58%), and also from other members of the multidrug resistance family such as ABCB1 (Pgp) which exhibited significant stimulation of their ATPase activity by these compounds. These results indicate that ABCC3 is not likely to play a major role in resistance to cancer drugs.

Kinetics of ATP Hydrolysis of ABCC3. Kinetic parameters of ATP hydrolysis were determined after activation of the purified protein with egg PC lipids. We observed maximal ATP hydrolysis by ABCC3 at concentrations of $\geq$10 mM MgATP with a V_{max} of 90 nmol min^{-1} mg^{-1} (k_{cat} = 0.26 s^{-1} or 16 min^{-1}) in the absence of taurocholate and a V_{max} of 210 nmol min^{-1} mg^{-1} (k_{cat} = 0.62 s^{-1} or 37 min^{-1}) in the presence of taurocholate. The K_m for MgATP was relatively high ($\sim$2 mM) and did not change in the absence or presence of taurocholate (Figure 8) or in the presence of ethinylestradiol-3G (data not shown). The best fit of the data was obtained using the Michaelis−Menten equation (solid lines in Figure 8); thus, cooperativity between the two NBDs was not apparent in ATP hydrolysis assays.

Divalent metal ions are essential cofactors for ATP hydrolysis by ABCC3 since no activity was detected in their absence (and presence of 5 mM EDTA). Although Mn^{2+}, Ca^{2+}, and Co^{2+} all supported ATP hydrolysis, the relative ATPase activity in the presence of those ions was lower than that with Mg^{2+}, yielding $\sim$17, $\sim$7, and 6% of the MgATP hydrolysis rate, respectively, when assayed at Me^{2+}ATP

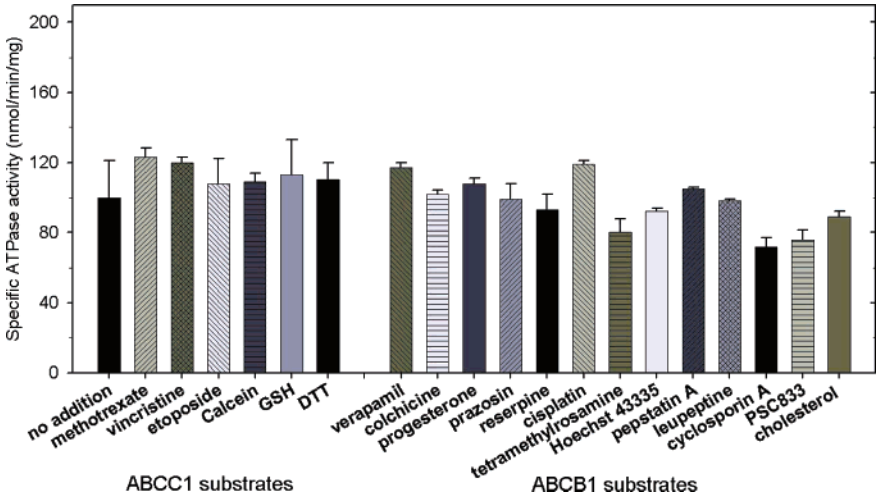

FIGURE 7: Stimulation of the ABCC3 ATPase by anticancer drugs. ATPase activity was assayed as described in the legend of Figure 5. Compounds were added from stocks in dimethyl sulfoxide with the final concentration of the solvent being ≤2% (v/v) in the assays. The same concentration of dimethyl sulfoxide had no effect on the ATPase activity of purified ABCC3 (data not shown). The bar graphs are the mean values obtained from at least three independent experiments ± standard deviations.

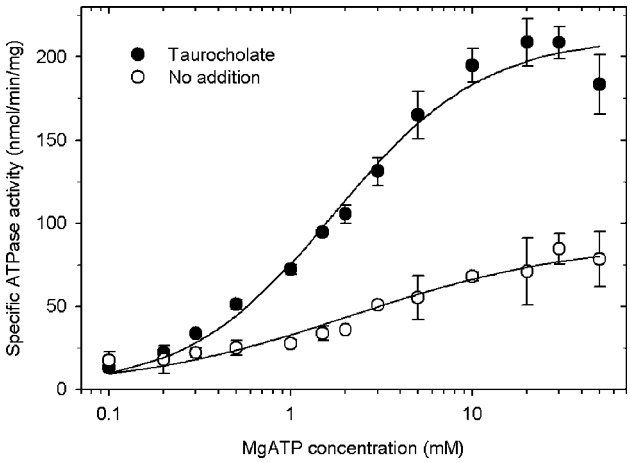

FIGURE 8: MgATP dependence of hydrolysis of purified ABCC3. Purified ABCC3 was activated with egg PC lipids and assayed with increasing concentrations of MgATP for 30 min at 37 °C in the absence or presence of 1 mM taurocholate. The lines in each case are a fit to the Michaelis−Menten equation expected for simple, noncooperative binding. The figure shows the average and standard deviation from two independent experiments.

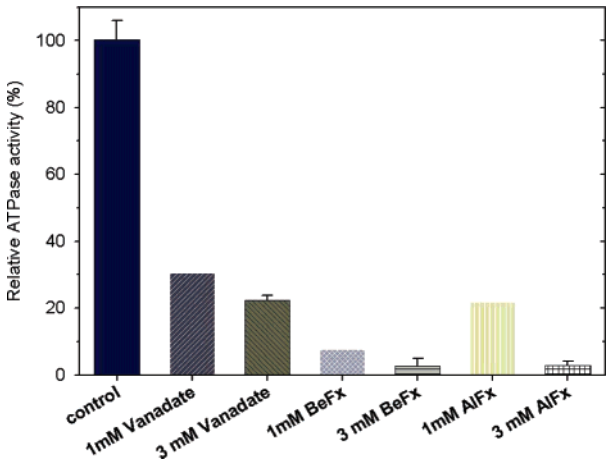

FIGURE 9: Inhibition of ATPase activity of ABCC3 by phosphate analogues. Purified ABCC3 was activated with egg PC lipids and ATPase activity assayed in the presence of 1 mM taurocholate for 15 min at 37 °C. The reaction cocktails contained 10 mM MgATP and inhibitors at a final concentration of 1 or 3 mM. One hundred percent activity (in the absence of inhibitor) was 180 ± 5 nmol min^{-1} mg^{-1}. The data are means of at least four independent experiments.

concentrations of 10 mM. MgATP hydrolysis in the presence of Mg^{2+} exhibited a broad pH optimum between 7.0 and 9.0 (Figure S2). Finally, we used transition and ground state analogues of phosphate (*22*) to monitor the inhibition of ATP hydrolysis (Figure 9). BeFx and AlFx were very effective, inhibiting ATPase activity by >90% at concentrations of 1 and 3 mM, respectively. With vanadate, complete inhibition was not achieved even at concentrations up to 3 mM, although the residual activity was small (31% at 1 mM and 22% at 3 mM). The incomplete inhibition by vanadate indicates that the coordination around the γ-phosphate during hydrolysis of ATP is somewhat less tight in ABCC3 than in Pgp which was completely inhibited at concentrations of 200 μM by this transition state analogue (*22*).

DISCUSSION

In this work, we present a comprehensive approach to cloning, expression, and purification of human ABC transporters in the yeast *P. pastoris*. We have inserted genes encoding 25 different human ABC transporters (52% of the total known) into expression vectors and analyzed their expression in membrane preparations of *P. pastoris* cells (Figure 2). Eleven of these transporters were expressed at levels comparable to, or higher than, the level of ABCB1 (Table S1), for which we routinely obtain homogeneous fully functional protein in yields of ~3−5 mg/100 g of wet cells (*29*). The best expressers included full-size transporter ABCC3, half-size transporters ABCB6, ABCD1, ABCG1, ABCG4, ABCG5, and ABCG8, and the four members of subfamilies E and F. We anticipate that these ABC transporters can be purified in yields similar to or higher than that of ABCB1 and thus that the yeast *P. pastoris* can provide ample material for their future biochemical and biophysical characterization.

We further demonstrate that in *P. pastoris*, as in many other host systems, the expression levels of individual recombinant gene products vary. Five ABC transporters (ABCA1, ABCA4, ABCC10, ABCC11, and ABCC12) were

expressed at levels lower than that of ABCB1 but were readily detectable on Western blots, while the remaining proteins either were below detection levels or produced truncated proteins (Table S1). Factors that affect the expression of these proteins may include the stability of the mRNAs, suboptimal codon usage of human genes for expression in yeast, and the susceptibility of individual gene products to proteolytic degradation possibly because of incorrect folding or subcellular targeting (*43*). These factors obviously differ among individual transporters, and since they cannot be predicted, they need to be determined experimentally for each protein of interest. In some cases, simple modifications of the growth conditions (e.g., media, pH, temperature, etc.) may be sufficient to improve expression. One example of such a successful optimization is the mitochondrial transporter ABCB7. We have observed that expression of ABCB7 from a constitutive promoter (*GAP* instead of *AOX1*) and a change of the growth medium proved to be advantageous for production of the fully processed transporter (M. Chloupková, unpublished observations). Another example is the case of the half-size transporters ABCG5 and ABCG8, which appear to function as heterodimers (*37*). Coexpression of these gene products significantly increases yields of purified proteins (~9 mg/100 g of cells), thus indicating that the two transporters stabilize each other during cell growth and subsequent copurification. Taken together, our results demonstrate that a number of human ABC transporters can be readily expressed in *P. pastoris*. For others which are not readily expressed in this system, the data presented in this study may serve as a starting point for the development of strategies for further enhancement of expression, if large-scale production of a particular gene becomes desirable.

Purification of ABC transporters in their active form, as for any large integral membrane protein, is a challenging task, although a variety of experimental strategies have been used previously. Since *P. pastoris* relies on high biomass production rather than "over"-expression of proteins, we added a tandem affinity tag to the open reading frame of all proteins to allow for a universally applicable approach for purification. As an example of the proposed strategy, we have purified, for the first time, the full-size transporter ABCC3 (Figure 3). We demonstrate that the purified protein, in the presence of lipids, exhibits high ATPase activity [82 ± 32 nmol min^{-1} mg^{-1} (Table 1)] comparable to those of the previously characterized transporters ABCC1 (5−10 nmol min^{-1} mg^{-1}) (*38*), ABCC2 (25 nmol min^{-1} mg^{-1}) (*39*), and ABCC7 (CFTR, 60 nmol min^{-1} mg^{-1}) (*19*, *40*). Furthermore, the ATPase activity of ABCC3 was stimulated by compounds that have been shown to be transported by ABCC3 in various systems (see below), thus providing convincing evidence that the purified protein is functional. Making use of the purified material, we were able for the first time to examine the substrate preference of ABCC3 in the absence of related transporters with overlapping substrate specificities, providing an interesting comparison to previous characterizations of this ABC transporter.

ABCC3 was originally expected to transport a broad spectrum of anticancer drugs and to contribute to multidrug resistance of human cancers, based on the fact that it is a member of the family of multidrug resistance (MDR) ABC transporters. This family is comprised of nine proteins of subfamily C [MRP1−9 (Table S1)] that are involved in detoxification of cells by exporting organic anions and conjugated anionic metabolites, as well as ABCB1 (MDR1, Pgp) and ABCG2 (BCRP) proteins which transport uncharged or positively charged hydrophobic compounds. Binding of substrate to the TMDs of ABC transporters typically stimulates ATP hydrolysis at the NBDs so that energy from the hydrolysis can be used to drive transport across membranes (*2*). The activities of ABCC1 and ABCC2 are stimulated ~1.5-fold (*44*) and ~2−3.5-fold (*39*) in the presence of transport substrates, and stimulation of up to 10-fold by substrates was observed in the case of ABCB1 (*28*). However, contrary to expectations, none of the 18 diverse compounds that are known substrates of both ABCC1 and ABCB1 exhibited any significant ability to stimulate the ATPase activity of ABCC3 (Figure 7). The tested compounds included methotrexate, etoposide, vincristine, and cisplatin, drugs for which resistance has been reported to be conferred by ABCC3 in transfected cell lines and in a panel of ABCC3-expressing human lung cancer lines (*45*, *46*). Despite this evidence, however, the question of whether ABCC3 is an MDR transporter has been under intense debate for the following reasons. (i) Methotrexate caused only a short-term, high-dose resistance (*47*) consistent with its low affinity for this drug in vesicular transport assays (*48*). (ii) In continuous exposure experiments, only low-level resistance to etoposide and tenoposide was found in the ABCC3-expressing cells but not to other drugs (*45*, *47*, *49*). (iii) *Abcc3*−/− mice did not reveal any increased chemosensitivity to etoposide in contrast to *Abcc1*−/− mice which did exhibit pronounced sensitivity to this drug (*50*, *51*). A possible explanation for the observed phenotypes is that the presence of other transporters with overlapping substrate specificities such as ABCC1 and ABCC2 may have masked the true effects of ABCC3 overexpression and/or mutation. Overall, our data obtained with purified ABCC3 agree with the in vivo findings questioning the role of ABCC3 in drug resistance and confirm that a variety of common anticancer drugs are not the preferred substrates for this transporter.

ABCC3 resides at the basolateral membrane of epithelial cells in the liver, gall bladder, gut, pancreas, kidney, and adrenal gland (*31*, *52*). In humans, the protein is overexpressed in patients with cholestasis and Dubin-Johnson syndrome (caused by mutations in *ABCC2*) (*31*). Therefore, it has been suggested that ABCC3 functions as a route for escape of bile acids and endobiotics into the blood for subsequent urinary secretion, preventing liver damage under conditions of impaired bile flow (*31*). However, whether human ABCC3 indeed transports free bile acids in vivo is still a matter of debate. We found that the ATPase activity of purified human ABCC3 was significantly stimulated by bile acids such as cholate, deoxycholate, glycocholate, and taurocholate in a concentration-dependent manner with maximum stimulation observed at ~1 mM (Figure 5). However, the concentration required for half-maximal stimulation (K_m) was relatively high (≥130 μM), and almost no stimulation was seen below 50 μM. These findings are consistent with a role of ABCC3 in cholestasis when concentrations of bile acids are high (up to millimolar) but not in the normal enterohepatic circulation of bile acids (*41*, *53*, *54*). In mouse and rat models, large amounts of bile acids accumulate in serum, liver, and other organs after bile duct

ligation to induce cholestasis (*32*). In *Abcc3*-deficient mice, significantly higher levels of bile acids such as taurocholate and tauro-β-muricholate accumulated in the liver after bile duct ligation (1.5-fold higher than in wild-type mice) (*41*, *52*). However, no abnormalities were observed in the bile acid concentration in serum of *Abcc3*-deficient mice. This may be attributed to a lack of inducibility of Abcc3 expression in certain mouse strains (*32*) in contrast to human patients with cholestasis (*31*). Direct transport assays using rat and human ABCC3 membrane vesicle systems have shown that taurocholate, glycocholate, and other bile acids are transported by this pump, albeit with low affinity and with apparent species-dependent specificities (reviewed in ref *32*). It may be noted that transport assays in membrane vesicles or whole cell systems generally are conducted at very low concentrations (*55*−*57*), e.g., significantly below the K_m values found in our experiments. Thus, differences in the affinities may explain the apparent lack of transport of taurocholate seen for human ABCC3 in contrast to rat Abcc3 (*56*); nevertheless, these observations are consistent with the low affinity of the human pump for free bile acids that we observe.

Recently, significantly reduced levels of glucuronide conjugates (-G) such as bilirubin-G, acetaminophenon-G, and morphine-G were observed in the serum of *Abcc3*−/− mice, suggesting that conjugated metabolites are the true transport substrates of Abcc3 (*41*, *52*, *58*, *59*). Therefore, we tested a variety of glucuronated conjugates[2] for their effects on the ATPase activity of purified human ABCC3 (Figure 5B). We found that they all stimulated the ATPase with half-maximal stimulation (K_m) seen at the relatively low concentrations of 2 and 3 μM in the cases of $E_2$17βG and EE-G, respectively (Figure 6B). These K_m values are in a range similar to those reported from transport assays of rat and human ABCC3 (reviewed in ref *32*). Thus, the affinity of ACBC3 for these glucuronated substrates is at least 10−100-fold higher than for free bile acids, indicating that they are the preferred substrates for this pump. Our observation that all the glucuronide conjugates stimulated the ATPase activity of ABCC1 agrees with the localization of ABCC3 in tissues with high glucuronidating capacity, the phenotype of *Abcc3*−/− mice, and the elevated levels of urinary excretion of glucuronides during cholestasis in humans (*52*, *58*−*61*). Thus, our work clearly implies that ABCC3 could play an important role in the transport of glucuronide conjugates for detoxification of liver and other organs in vivo.

In conclusion, we have found that 11 human ABC transporters can be expressed in *P. pastoris* at levels providing sufficient amounts of purified material for biochemical and biophysical analyses. In addition, we purified the full-size transporter ABCC3 and characterized its ATPase with respect to stimulation by previously proposed transport substrates. The transporter exhibits low apparent affinities for free bile acids and much higher affinities for some glucuronide conjugates. Our work thus aids in the understanding of the biological role of ABCC3 and presents a major step toward structure−function analysis not only of ABCC3 but also of other human ABC transporters.

[2] The number of commercially available glucuronide conjugates is rather limited and does not include any glucuronated bile salts.

ACKNOWLEDGMENT

We are grateful to A. E. Senior for helpful discussions and Yadushyla Narasimhachar and Mandy Geryk for excellent technical assistance.

SUPPORTING INFORMATION AVAILABLE

A summary of the expression analysis of 25 human ABC transporters (Table S1), expression analysis of ABCB1 in different vectors (Figure S1), and a pH profile of the ATP hydrolysis of ABCC3 (Figure S2). This material is available free of charge via the Internet at http://pubs.acs.org.

REFERENCES

1. Dean, M., and Allikmets, R. (2001) Complete characterization of the human ABC gene family, *J. Bioenerg. Biomembr. 33*, 475−479.
2. Holland, I. B., and Blight, M. A. (1999) ABC-ATPases, adaptable energy generators fuelling transmembrane movement of a variety of molecules in organisms from bacteria to humans, *J. Mol. Biol. 293*, 381−399.
3. Hanekop, N., Zaitseva, J., Jenewein, S., Holland, I. B., and Schmitt, L. (2006) Molecular insights into the mechanism of ATP-hydrolysis by the NBD of the ABC-transporter HlyB, *FEBS Lett. 580*, 1036−1041.
4. Gadsby, D. C., Vergani, P., and Csanady, L. (2006) The ABC protein turned chloride channel whose failure causes cystic fibrosis, *Nature 440*, 477−483.
5. Abele, R., and Tampe, R. (2006) Modulation of the antigen transport machinery TAP by friends and enemies, *FEBS Lett. 580*, 1156−1163.
6. Klaver, C. C., and Allikmets, R. (2003) Genetics of macular dystrophies and implications for age-related macular degeneration, *Dev. Ophthalmol. 37*, 155−169.
7. Allikmets, R., Raskind, W. H., Hutchinson, A., Schueck, N. D., Dean, M., and Koeller, D. M. (1999) Mutation of a putative mitochondrial iron transporter gene (ABC7) in X-linked sideroblastic anemia and ataxia (XLSA/A), *Hum. Mol. Genet. 8*, 743−749.
8. Takahashi, K., Kimura, Y., Nagata, K., Yamamoto, A., Matsuo, M., and Ueda, K. (2005) ABC proteins: Key molecules for lipid homeostasis, *Med. Mol. Morphol. 38*, 2−12.
9. von Bergmann, K., Sudhop, T., and Lutjohann, D. (2005) Cholesterol and plant sterol absorption: Recent insights, *Am. J. Cardiol. 96*, 10D−14D.
10. Borst, P., and Elferink, R. O. (2002) Mammalian ABC transporter in health and disease, *Annu. Rev. Biochem. 71*, 537−592.
11. Szakacs, G., Paterson, J. K., Ludwig, J. A., Booth-Genthe, C., and Gottesman, M. M. (2006) Targeting multidrug resistance in cancer, *Nat. Rev. Drug Discovery 5*, 219−234.
12. Oswald, C., Holland, I. B., and Schmitt, L. (2006) The motor domains of ABC-transporters. What can structures tell us? *Naunyn-Schmiedebergs Arch. Pharmakol. 372*, 385−399.
13. Locher, K. P., Lee, A. T., and Rees, D. C. (2002) The *E. coli* BtuCD structure: A framework for ABC transporter architecture and mechanism, *Science 296*, 1091−1098.
14. Dawson, R. J., and Locher, K. P. (2006) Structure of a bacterial multidrug ABC transporter, *Nature 443*, 180−185.
15. Pinkett, H. W., Lee, A. T., Lum, P., Locher, K. P., and Rees, D. C. (2007) An inward-facing conformation of a putative metal-chelate-type ABC transporter, *Science 315*, 373−377.
16. Hollenstein, K., Frei, D. C., and Locher, K. P. (2007) Structure of an ABC transporter in complex with its binding protein, *Nature 446*, 213−216.
17. Lee, J. Y., Urbatsch, I. L., Senior, A. E., and Wilkens, S. (2002) Projection structure of P-glycoprotein by electron microscopy. Evidence for a closed conformation of the nucleotide binding domains, *J. Biol. Chem. 277*, 40125−40131.
18. Rosenberg, M. F., Callaghan, R., Modok, S., Higgins, C. F., and Ford, R. C. (2005) Three-dimensional structure of P-glycoprotein: The transmembrane regions adopt an asymmetric configuration in the nucleotide-bound state, *J. Biol. Chem. 280*, 2857−2862.
19. Rosenberg, M. F., Kamis, A. B., Aleksandrov, L. A., Ford, R. C., and Riordan, J. R. (2004) Purification and crystallization of the

cystic fibrosis transmembrane conductance regulator (CFTR), *J. Biol. Chem. 279*, 39051−39057.
20. Rosenberg, M. F., Velarde, G., Ford, R. C., Martin, C., Berridge, G., Kerr, I. D., Callaghan, R., Schmidlin, A., Wooding, C., Linton, K. J., and Higgins, C. F. (2001) Repacking of the transmembrane domains of P-glycoprotein during the transport ATPase cycle, *EMBO J. 20*, 5615−5625.
21. McDevitt, C. A., Collins, R. F., Conway, M., Modok, S., Storm, J., Kerr, I. D., Ford, R. C., and Callaghan, R. (2006) Purification and 3D structural analysis of oligomeric human multidrug transporter ABCG2, *Structure 14*, 1623−1632.
22. Urbatsch, I. L., Tyndall, G. A., Tombline, G., and Senior, A. E. (2003) P-Glycoprotein catalytic mechanism: Studies of the ADP-vanadate inhibited state, *J. Biol. Chem. 278*, 23171−23179.
23. Deeley, R. G., and Cole, S. P. (2006) Substrate recognition and transport by multidrug resistance protein 1 (ABCC1), *FEBS Lett. 580*, 1103−1111.
24. Figler, R. A., Omote, H., Nakamoto, R. K., and Al-Shawi, M. K. (2000) Use of chemical chaperones in the yeast *Saccharomyces cerevisiae* to enhance heterologous membrane protein expression: High-yield expression and purification of human P-glycoprotein, *Arch. Biochem. Biophys. 376*, 34−46.
25. Ramachandra, M., Ambudkar, S. V., Gottesman, M. M., Pastan, I., and Hrycyna, C. A. (1996) Functional characterization of a glycine 185-to-valine substitution in human P-glycoprotein by using a vaccinia-based transient expression system, *Mol. Biol. Cell 7*, 1485−1498.
26. Sarkadi, B., Price, E. M., Boucher, R. C., Germann, U. A., and Scarborough, G. A. (1992) Expression of the human multidrug resistance cDNA in insect cells generates a high activity drug-stimulated membrane ATPase, *J. Biol. Chem. 267*, 4854−4858.
27. Linton, K. J., and Higgins, C. F. (2002) P-Glycoprotein misfolds in *Escherichia coli*: Evidence against alternating-topology models of the transport cycle, *Mol. Membr. Biol. 19*, 51−58.
28. Lerner-Marmarosh, N., Gimi, K., Urbatsch, I. L., Gros, P., and Senior, A. E. (1999) Large scale purification of detergent-soluble P-glycoprotein from *Pichia pastoris* cells and characterization of nucleotide binding properties of wild-type, Walker A, and Walker B mutant proteins, *J. Biol. Chem. 274*, 34711−34718.
29. Urbatsch, I. L., Gimi, K., Wilke-Mounts, S., Lerner-Marmarosh, N., Rousseau, M. E., Gros, P., and Senior, A. E. (2001) Cysteines 431 and 1074 are responsible for inhibitory disulfide cross-linking between the two nucleotide-binding sites in human P-glycoprotein, *J. Biol. Chem. 276*, 26980−26987.
30. Urbatsch, I. L., Wilke-Mounts, S., Gimi, K., and Senior, A. E. (2001) Purification and characterization of N-glycosylation mutant mouse and human P-glycoproteins expressed in *Pichia pastoris* cells, *Arch. Biochem. Biophys. 388*, 171−177.
31. Scheffer, G. L., Kool, M., de Haas, M., de Vree, J. M., Pijnenborg, A. C., Bosman, D. K., Elferink, R. P., van der Valk, P., Borst, P., and Scheper, R. J. (2002) Tissue distribution and induction of human multidrug resistant protein 3, *Lab. Invest. 82*, 193−201.
32. Borst, P., de Wolf, C., and van de Wetering, K. (2006) Multidrug resistance-associated proteins 3, 4, and 5, *Pfluegers Arch.* (in press).
33. Doyle, S. A. (2005) High-throughput cloning for proteomics research, *Methods Mol. Biol. 310*, 107−113.
34. Aslanidis, C., de Jong, P. J., and Schmitz, G. (1994) Minimal length requirement of the single-stranded tails for ligation-independent cloning (LIC) of PCR products, *PCR Methods Appl. 4*, 172−177.
35. Li, C., and Evans, R. M. (1997) Ligation independent cloning irrespective of restriction site compatibility, *Nucleic Acids Res. 25*, 4165−4166.
36. Urbatsch, I. L., Beaudet, L., Carrier, I., and Gros, P. (1998) Mutations in either nucleotide-binding site of P-glycoprotein (Mdr3) prevent vanadate trapping of nucleotide at both sites, *Biochemistry 37*, 4592−4602.
37. Wang, Z., Stalcup, L. D., Harvey, B. J., Weber, J., Chloupkova, M., Dumont, M. E., Dean, M., and Urbatsch, I. L. (2006) Purification and ATP hydrolysis of the putative cholesterol transporters ABCG5 and ABCG8, *Biochemistry 45*, 9929−9939.
38. Mao, Q., Deeley, R. G., and Cole, S. P. (2000) Functional reconstitution of substrate transport by purified multidrug resistance protein MRP1 (ABCC1) in phospholipid vesicles, *J. Biol. Chem. 275*, 34166−34172.
39. Hagmann, W., Nies, A. T., Konig, J., Frey, M., Zentgraf, H., and Keppler, D. (1999) Purification of the human apical conjugate export pump MRP2 reconstitution and functional characterization as substrate-stimulated ATPase, *Eur. J. Biochem. 265*, 281−289.
40. Ketchum, C. J., Rajendrakumar, G. V., and Maloney, P. C. (2004) Characterization of the adenosinetriphosphatase and transport activities of purified cystic fibrosis transmembrane conductance regulator, *Biochemistry 43*, 1045−1053.
41. Belinsky, M. G., Dawson, P. A., Shchaveleva, I., Bain, L. J., Wang, R., Ling, V., Chen, Z. S., Grinberg, A., Westphal, H., Klein-Szanto, A., Lerro, A., and Kruh, G. D. (2005) Analysis of the in vivo functions of Mrp3, *Mol. Pharmacol. 68*, 160−168.
42. Kruh, G. D., and Belinsky, M. G. (2003) The MRP family of drug efflux pumps, *Oncogene 22*, 7537−7552.
43. Daly, R., and Hearn, M. T. (2005) Expression of heterologous proteins in *Pichia pastoris*: A useful experimental tool in protein engineering and production, *J. Mol. Recognit. 18*, 119−138.
44. Mao, Q., Leslie, E. M., Deeley, R. G., and Cole, S. P. (1999) ATPase activity of purified and reconstituted multidrug resistance protein MRP1 from drug-selected H69AR cells, *Biochim. Biophys. Acta 1461*, 69−82.
45. Zeng, H., Bain, L. J., Belinsky, M. G., and Kruh, G. D. (1999) Expression of multidrug resistance protein-3 (multispecific organic anion transporter-D) in human embryonic kidney 293 cells confers resistance to anticancer agents, *Cancer Res. 59*, 5964−5967.
46. Young, L. C., Campling, B. G., Cole, S. P., Deeley, R. G., and Gerlach, J. H. (2001) Multidrug resistance proteins MRP3, MRP1, and MRP2 in lung cancer: Correlation of protein levels with drug response and messenger RNA levels, *Clin. Cancer Res. 7*, 1798−1804.
47. Kool, M., van der Linden, M., de Haas, M., Scheffer, G. L., de Vree, J. M., Smith, A. J., Jansen, G., Peters, G. J., Ponne, N., Scheper, R. J., Elferink, R. P., Baas, F., and Borst, P. (1999) MRP3, an organic anion transporter able to transport anti-cancer drugs, *Proc. Natl. Acad. Sci. U.S.A. 96*, 6914−6919.
48. Zeng, H., Chen, Z. S., Belinsky, M. G., Rea, P. A., and Kruh, G. D. (2001) Transport of methotrexate (MTX) and folates by multidrug resistance protein (MRP) 3 and MRP1: Effect of polyglutamylation on MTX transport, *Cancer Res. 61*, 7225−7232.
49. Zelcer, N., Saeki, T., Reid, G., Beijnen, J. H., and Borst, P. (2001) Characterization of drug transport by the human multidrug resistance protein 3 (ABCC3), *J. Biol. Chem. 276*, 46400−46407.
50. Lorico, A., Rappa, G., Finch, R. A., Yang, D., Flavell, R. A., and Sartorelli, A. C. (1997) Disruption of the murine MRP (multidrug resistance protein) gene leads to increased sensitivity to etoposide (VP-16) and increased levels of glutathione, *Cancer Res. 57*, 5238−5242.
51. Wijnholds, J., Evers, R., van Leusden, M. R., Mol, C. A., Zaman, G. J., Mayer, U., Beijnen, J. H., van der Valk, M., Krimpenfort, P., and Borst, P. (1997) Increased sensitivity to anticancer drugs and decreased inflammatory response in mice lacking the multidrug resistance-associated protein, *Nat. Med. 3*, 1275−1279.
52. Zelcer, N., van de Wetering, K., de Waart, R., Scheffer, G. L., Marschall, H. U., Wielinga, P. R., Kuil, A., Kunne, C., Smith, A., van der Valk, M., Wijnholds, J., Elferink, R. O., and Borst, P. (2006) Mice lacking Mrp3 (Abcc3) have normal bile salt transport, but altered hepatic transport of endogenous glucuronides, *J. Hepatol. 44*, 768−775.
53. Panveliwalla, D., Lewis, B., Wootton, I. D., and Tabaqchali, S. (1970) Determination of individual bile acids in biological fluids by thin-layer chromatography and fluorimetry, *J. Clin. Pathol. 23*, 309−314.
54. Kruh, G. D., Belinsky, M. G., Gallo, J. M., and Lee, K. (2007) Physiological and pharmacological functions of Mrp2, Mrp3 and Mrp4 as determined from recent studies on gene-disrupted mice, *Cancer Metastasis Rev. 26*, 5−14.
55. Zelcer, N., Saeki, T., Bot, I., Kuil, A., and Borst, P. (2003) Transport of bile acids in multidrug-resistance-protein 3-overexpressing cells co-transfected with the ileal Na^+-dependent bile-acid transporter, *Biochem. J. 369*, 23−30.
56. Akita, H., Suzuki, H., Hirohashi, T., Takikawa, H., and Sugiyama, Y. (2002) Transport activity of human MRP3 expressed in Sf9 cells: Comparative studies with rat MRP3, *Pharm. Res. 19*, 34−41.
57. Zeng, H., Liu, G., Rea, P. A., and Kruh, G. D. (2000) Transport of amphipathic anions by human multidrug resistance protein 3, *Cancer Res. 60*, 4779−4784.

58. Zelcer, N., van de Wetering, K., Hillebrand, M., Sarton, E., Kuil, A., Wielinga, P. R., Tephly, T., Dahan, A., Beijnen, J. H., and Borst, P. (2005) Mice lacking multidrug resistance protein 3 show altered morphine pharmacokinetics and morphine-6-glucuronide antinociception, *Proc. Natl. Acad. Sci. U.S.A. 102*, 7274−7279.
59. Zamek-Gliszczynski, M. J., Nezasa, K., Tian, X., Bridges, A. S., Lee, K., Belinsky, M. G., Kruh, G. D., and Brouwer, K. L. (2006) Evaluation of the role of multidrug resistance-associated protein (mrp) 3 and mrp4 in hepatic basolateral excretion of sulfate and glucuronide metabolites of acetaminophen, 4-methylumbelliferone, and harmol in abcc3−/− and abcc4−/− mice, *J. Pharmacol. Exp. Ther. 319*, 1485−1491.
60. Manautou, J. E., de Waart, D. R., Kunne, C., Zelcer, N., Goedken, M., Borst, P., and Elferink, R. O. (2005) Altered disposition of acetaminophen in mice with a disruption of the Mrp3 gene, *Hepatology 42*, 1091−1098.
61. Wietholtz, H., Marschall, H. U., Reuschenbach, R., Matern, H., and Matern, S. (1991) Urinary excretion of bile acid glucosides and glucuronides in extrahepatic cholestasis, *Hepatology 13*, 656−662.
62. Cai, J., Daoud, R., Georges, E., and Gros, P. (2001) Functional expression of multidrug resistance protein 1 in *Pichia pastoris*, *Biochemistry 40*, 8307−8316.

BI700020M